TAO, Vol. 7, No. 4, 535-548, December 1996

Northern Luzon Arc: Location and Tectonic Features From Magnetic Data off Eastern Taiwan

Chuen-Tien Shyu[1], Mei-Chang Chih[1], Shu-Kun Hsu[1]
Chengsung Wang[2] and Boris Karp[3]

(Manuscript received 9 October 1996, in final form 28 November 1996)

ABSTRACT

Magnetic data collected from 1989 to 1994 off eastern Taiwan were analyzed for tectonic interpretation. Unlike what was previously believed, the magnetic features indicate that the northern Luzon Arc extends to the east of the Coastal Range. Accordingly, most of the Coastal Range and its southward extension (the Huatung Ridge) could be regarded as a compressed subduction complex. The northern Luzon Arc has changed in direction from NNW-SSE to NNE-SSW at the Taitung Canyon between the Lutao and Lanhsu Islands. The collision between the Luzon Arc and the Tananao Complex, which occurs north of 23.5°N, corresponds to a hard collision (with little or without buffered material in between) as evidenced by the intensive occurrence of earthquakes. South of 23.5°N, the collision between the Luzon Arc and the Tananao Complex is a soft one, buffered by the compressing subduction complex. The magnetic boundaries of the northern Luzon Arc divide the earthquakes into two main provinces, corresponding to hard collision and soft collision. North of 22.7°N, the Luzon Arc has been subsiding, which is probably associated with the northwestward subduction of the Philippine Sea plate beneath the northeastern Taiwan area.

(Key words: Magnetic anomaly, Northern Luzon Arc, Arc-arc collision)

1. INTRODUCTION

The Eurasian and the Philippine Sea plates are actively interacting in the Taiwan region (Figure 1). In the south of Taiwan, the lithosphere of the South China Sea subducts eastward beneath the Philippine Sea plate along the Manila Trench and creates the Luzon Arc. In the northeast of Taiwan, the Philippine Sea plate subducts beneath the Ryukyu Arc and creates the Okinawa Trough backarc basin. So far, two principal models have been put forth to explain the formation of Taiwan: the arc-continent collision (Suppe, 1981, 1984; Teng, 1990; Lu and Hsu, 1992) and the arc-arc collision (Hsu and Sibuet, 1995; Hsu *et al.*, 1996a). Between these

1 Institute of Oceanography, National Taiwan University, P.O. Box 23-13, Taipei, Taiwan, R.O.C.
2 Institute of Applied Geophysics, National Taiwan Ocean University, Taiwan, R.O.C.
3 Pacific Oceanological Institute, Russian Academy of Sciences

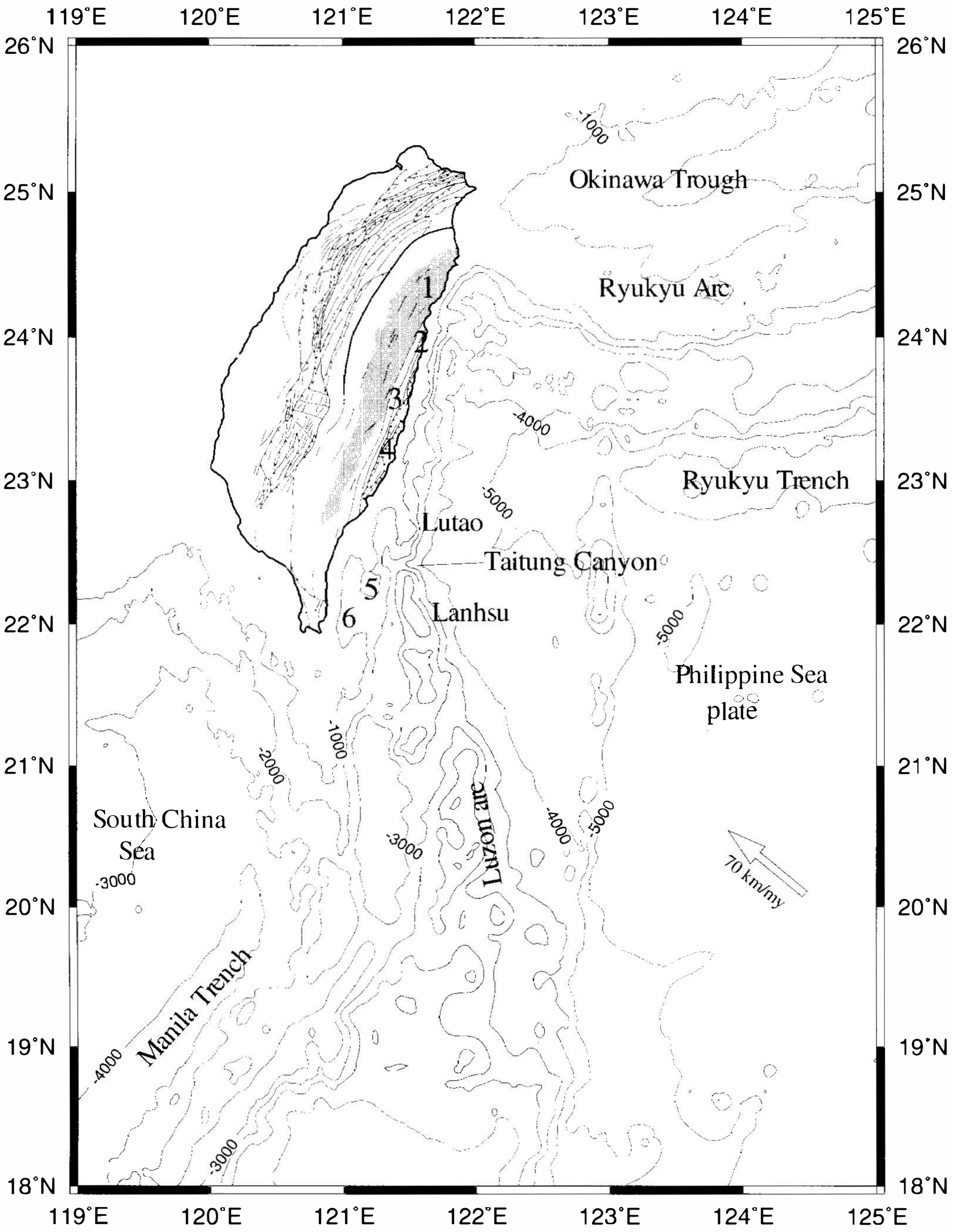

Fig. 1. Tectonic setting of Taiwan and its environs (after Hsu and Sibuet, 1995; Hsu *et al.*, 1996a). 1 = Tananao Complex; 2 = Hualien; 3 = Longitudinal Valley; 4 = Chengkung; 5 = Huatung Ridge; 6 = South Longitudinal Trough.

two models, however, a major contradiction as to the location of the suture exists between the Philippine Sea plate and the Eurasian plate. Teng (1990) concluded that the suture is located in western Taiwan and corresponds to the deformation front. Lu and Hsu (1992), on the other hand, proposed that the main suture is along the Lishan Fault and the Laonungchi Fault to the south. Hsu and Sibuet (1995) later suggested that the proto-Taiwan was located in a system of backarc basins that were younger and more active oceanward from the Late Cretaceous to Late Miocene (Sibuet and Hsu, 1996): the Tananao Complex corresponds to a portion of the former Ryukyu Arc before it collided with the Luzon Arc. Thus, according to Hsu and Sibuet's model, the suture between the Eurasian and the Philippine Sea plates or more exactly between the former Ryukyu Arc (Tananao Complex) and the Luzon Arc is located along the Longitudinal Valley. In fact, both the petrology (Kizaki, 1986) and seismic velocity structures (Cheng *et al.*, 1996) do demonstrate similarities between the Tananao Complex and the south Ryukyu Arc. Furthermore, the direction of the Lishan Fault is continuously in the prolongation of the Okinawa Trough axis. Accordingly, the Longitudinal Valley may well be more suitable as the suture of the plate boundary. However, the outline of the indenter (Luzon Arc) has not yet been clearly defined.

The Luzon Arc, south of 23.2°N, was not identified until 1991 (Shyu and Chen, 1991). The most obvious feature from their magnetic interpretation was the location of the Lutao-Lanhsu Ridge (a portion of the Luzon Arc) (Figure 2). However, this could lead to the conclusion that the northern portion of the Luzon Arc extends into the coast near Chengkung (Figures 1 and 2). Since 1991, more magnetic data have been collected in the eastern and northeastern offshore areas of Taiwan, which allows to define a more complete location of the northern portion of the Luzon Arc. The tectonic features of the northern Luzon Arc are discussed later in this paper.

2. BATHYMETRIC AND MAGNETIC MAPS

The bathymetric maps (Figures 3 and 7) were made available from the US National Geophysical Data Center (NGDC) and the Institute of Oceanography of National Taiwan University data banks. Magnetic data were compiled from cruises of the *R/V Ocean Researcher I* from 1989 to 1994 and two cruises of the R/V Professor Gagarinsky in 1994 (Figure 4). Tracking of the ships through the survey area were extended out from the eastern coast of Taiwan with the track spacing typically 6-8 km. Some tracks along the coast and in the north-south trend proved useful for cross-over correction. Magnetic field measurements were conducted by a proton magnetometer towed 200 m behind the ship. Navigation employed the Global Positioning System (GPS) and magnetic results were reported as magnetic anomalies in reference to the 1995 International Geomagnetic Reference Field model (Figure 5).

3. MAGNETIC FEATURES AND THEIR INTERPRETATIONS

The framed area of Figure 5 shows the total magnetic anomalies of the study area. A conspicuous feature of the magnetic anomaly, with trends changing from NNW-SSE to NNE-SSW at 22.5°N, is distributed along offshore eastern Taiwan from 21.2°N to 24°N. A positive correlation generally exists between the magnetic anomalies, bathymetric relieves and

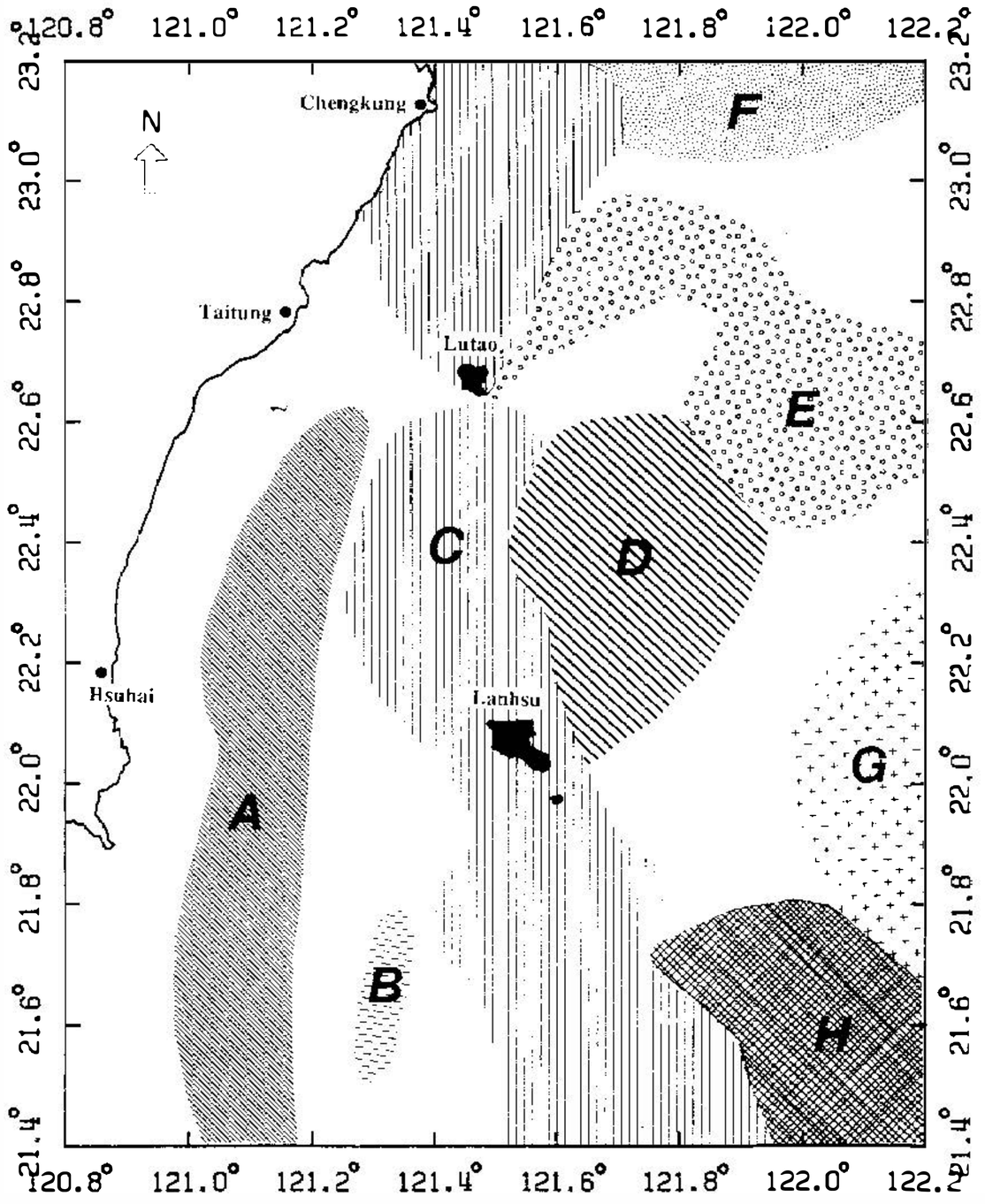

Fig. 2. Most obvious magnetic basement, Zone C, correlates well with the Lutao-Lanhsu Ridge and seems to go into Chengkung (after Shyu and Chen, 1991).

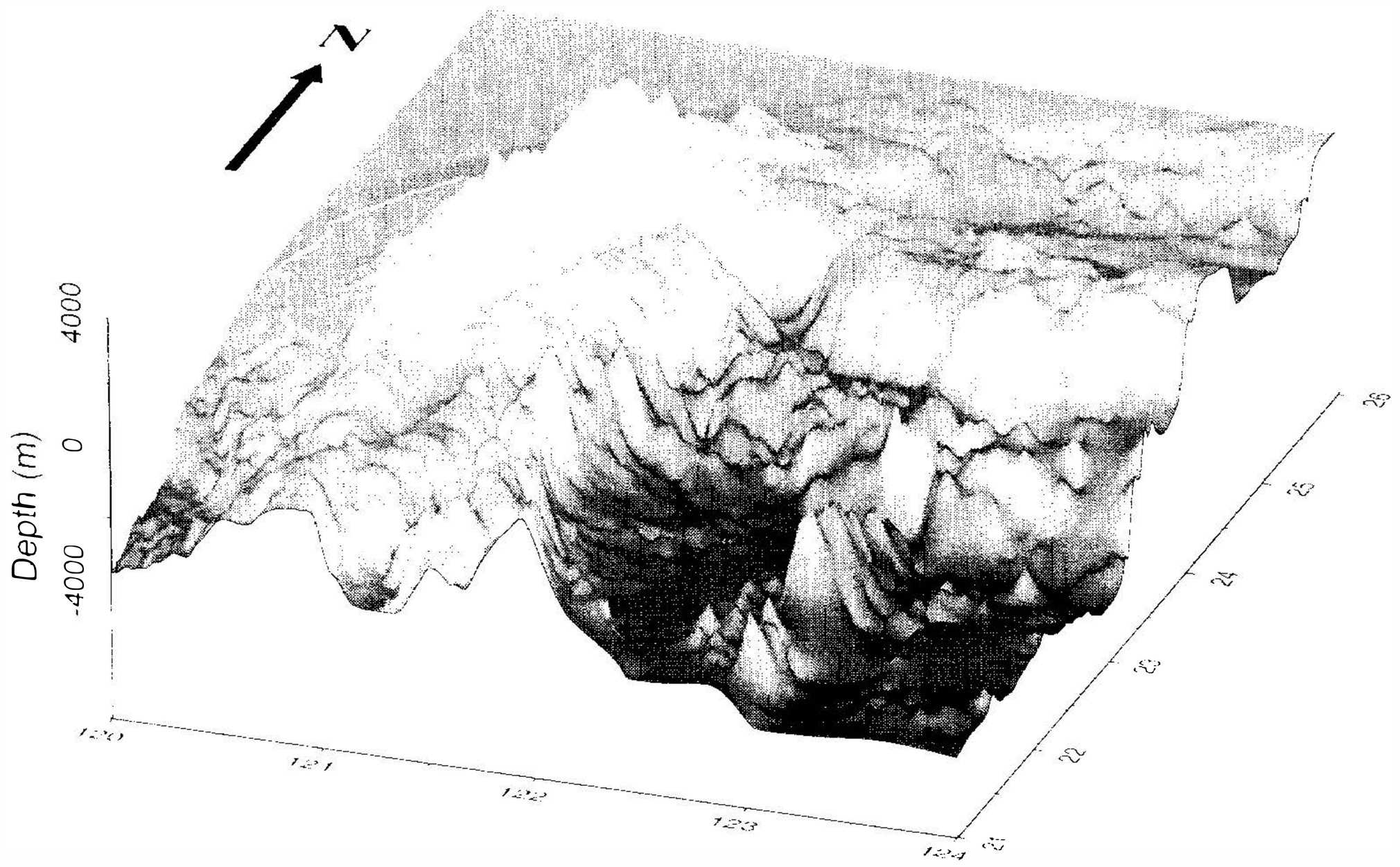

Fig. 3. Perspective view of the bathymetric map around Taiwan (data from Hsu *et al.*, 1996a).

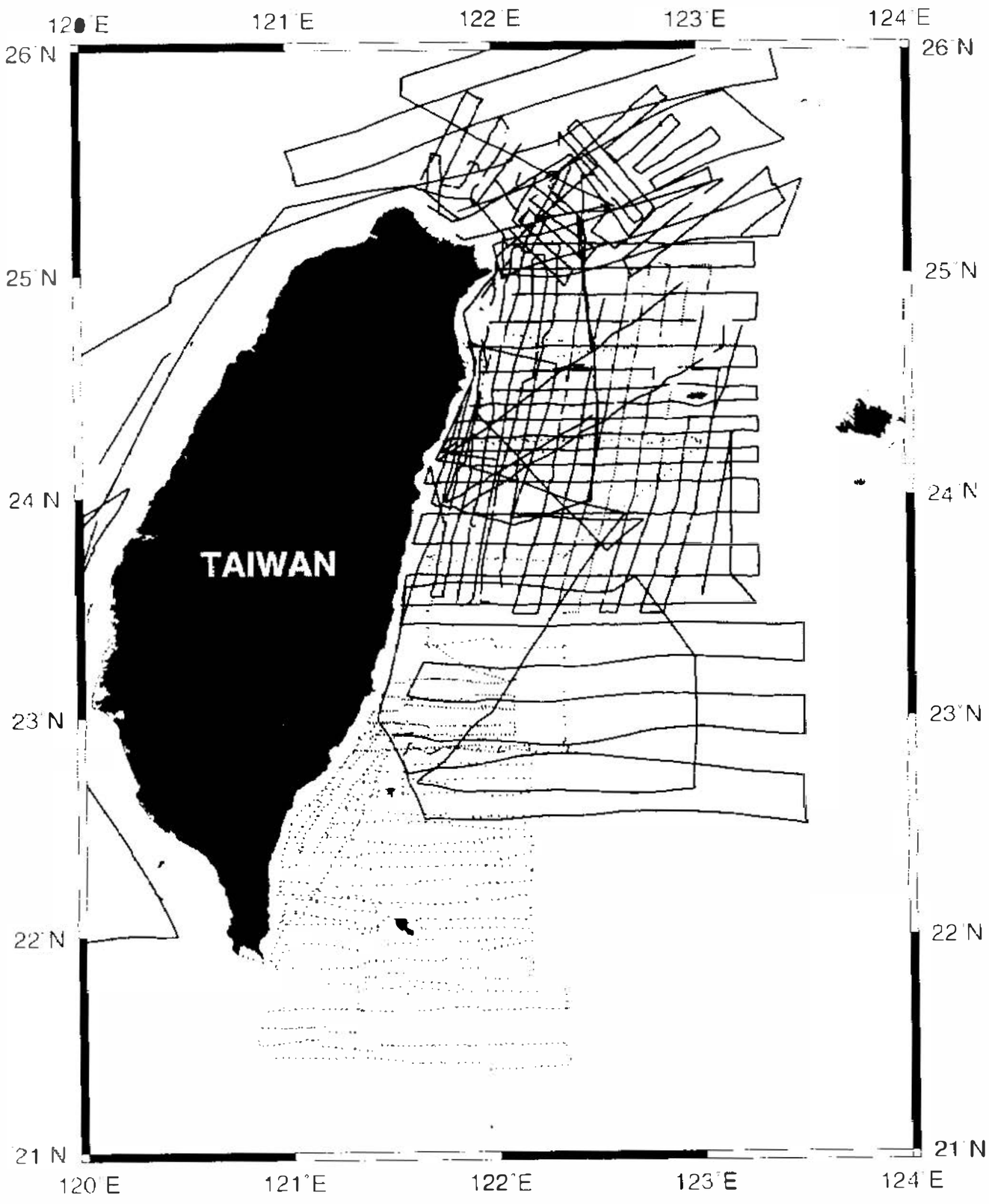

Fig. 4. Magnetic data along the ships' tracks and on the dotted positions which were used in this study.

volcanic rocks, the elongated positive magnetic anomaly off eastern Taiwan suggests that the Luzon Arc probably extends into the offshore region of the Coastal Range. In other words, from south to north the NNW-SSE trending magnetic anomaly of the Luzon Arc has turned to NNE-SSW at the place where the Taitung Canyon turns toward east.

The enhanced analytic signal technique developed to analyze potential field data (Hsu *et al.*, 1996b) was used in this study. It demonstrates the following advantages: 1) the interference effect between close anomalies is reduced; 2) the determined locations of maximum amplitudes of the analytic signal, corresponding to geological boundaries such as faults or contacts, are independent of ambient parameters such as inclination and declination of magnetization; and 3) the determination of maximum amplitudes can be automatically achieved by examining every 9-point grid-cell (Blakely and Simpson, 1986). The amplitudes of the second-order analytic signal for the study area are shown in Figure 6. The details of the used analytic signal technique is described in Hsu et al. (1996b).

With the automatically detected boundaries as revealed by the maximum amplitudes in Figure 6 as well as the morphological features in study area, several major faults or contacts (Figure 7) can be traced. Comparing the detected boundaries with the distribution of total magnetic intensity (Figure 5), the outline of the northern Luzon Arc (the gray areas in

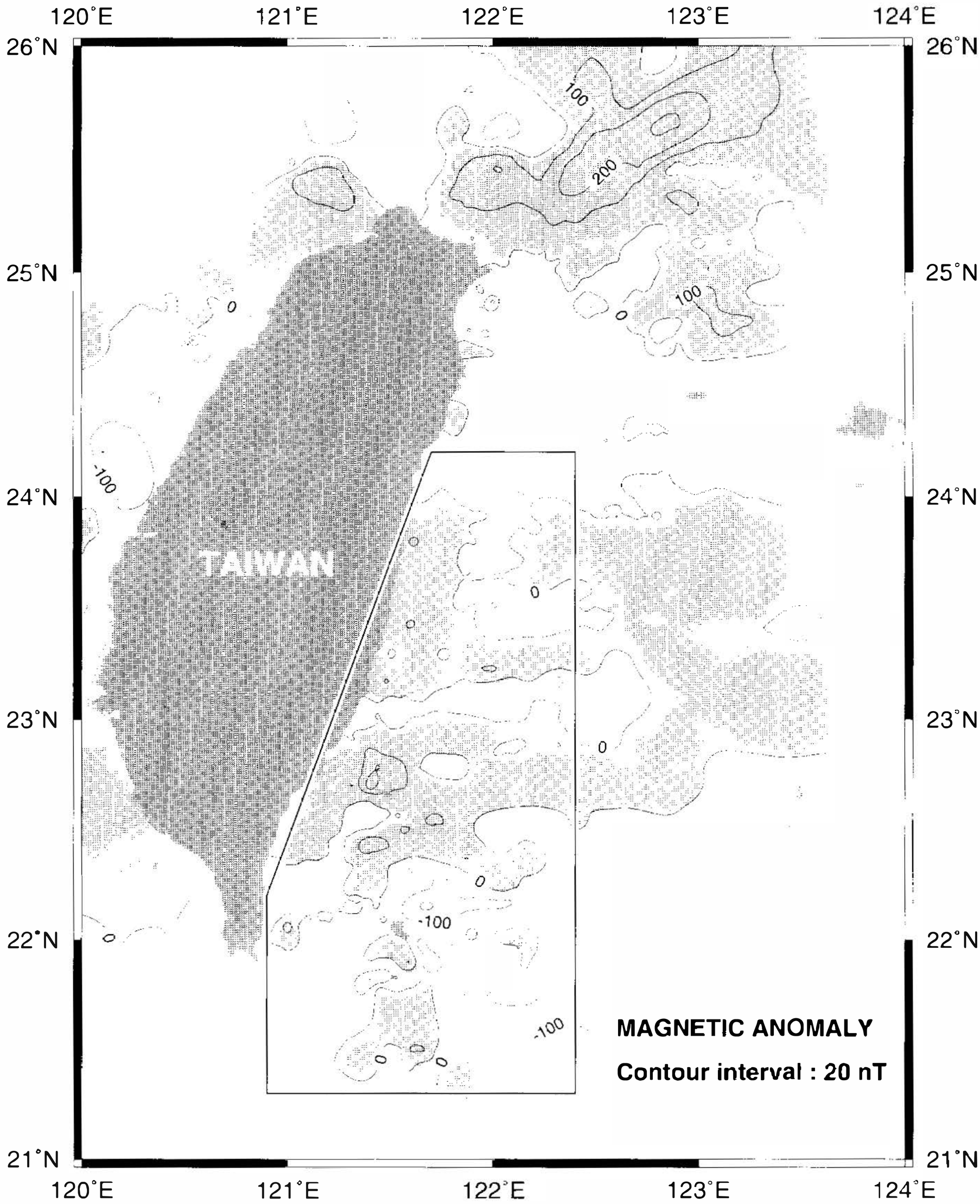

Fig. 5. Contours of total-field magnetic anomalies. Positive values are shaded. Anomalies in the framed area were used in this study.

Figure 7) can be delineated. However, the Luzon Arc may be larger in deeper areas. It should be noted that the northern Luzon Arc is, in fact, segmented into several blocks on account of the existence of fractures and/or faults. Two major portions of the northern Luzon Arc are separated by the Taitung Canyon which deepens eastward from about 2000 m to 4000 m. The turning point near the Taitung Canyon suggests a major stress change (Hsu *et al*, 1996a). The long and narrow portion trending NNE to the north of Lutao Island is believed to be the northernmost portion of the Luzon Arc. Instead of those depicted previously (e.g., Ho, 1988; Huang *et al*.,1992, 1995), the location of the Luzon Arc is, in general, apart from the eastern coast of

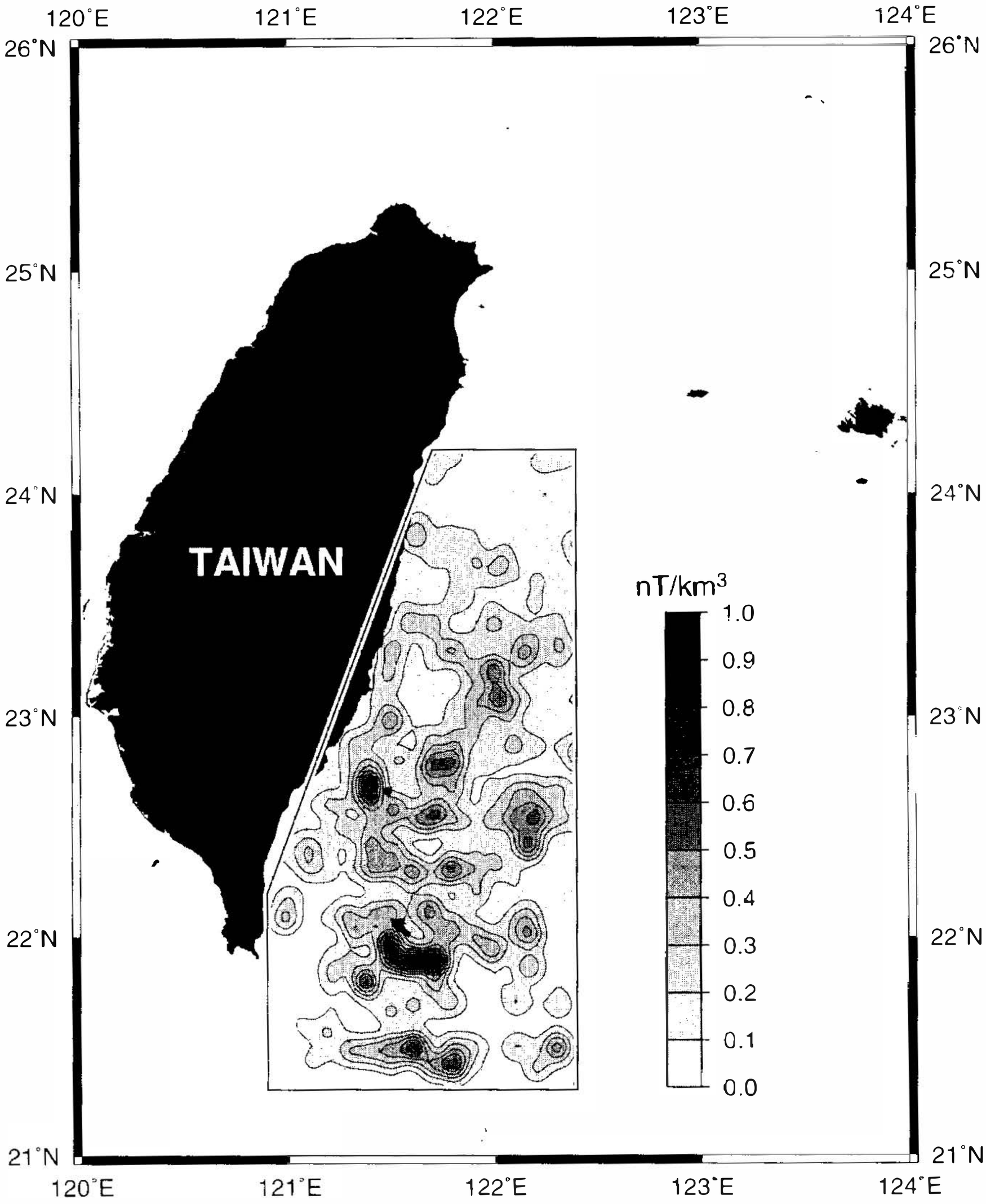

Fig. 6. Contours of amplitudes of the second-order enhanced analytic signal.

Taiwan. North of the Taitung Canyon, the arc is more or less along the continental slope with its northernmost portion impinging upon the Hualien coast and terminating near 24.18°N and 121.77°E where a major lineation trending NE-SW is detected (Figure 7). Therefore, most of the Coastal Range and its southward extension (the Huatung Ridge) can be regarded as a compressed and uplifted subduction complex (the hatched area in Figure 7). In other words, the Longitudinal Valley is suitable for the suture along the former Manila Trench, as proposed by Hsu and Sibuet (1995). The suture can also be extended southward along the South Longitudinal Trough in which a major magnetic boundary is detected (Figure 7). Farther south, the compressed subduction complex suffers probably a right-lateral fault, which is consistent with the analyses of GPS geodetic data (Yu *et al.*, 1995) and marine gravity data (Fuh *et al*, 1994).

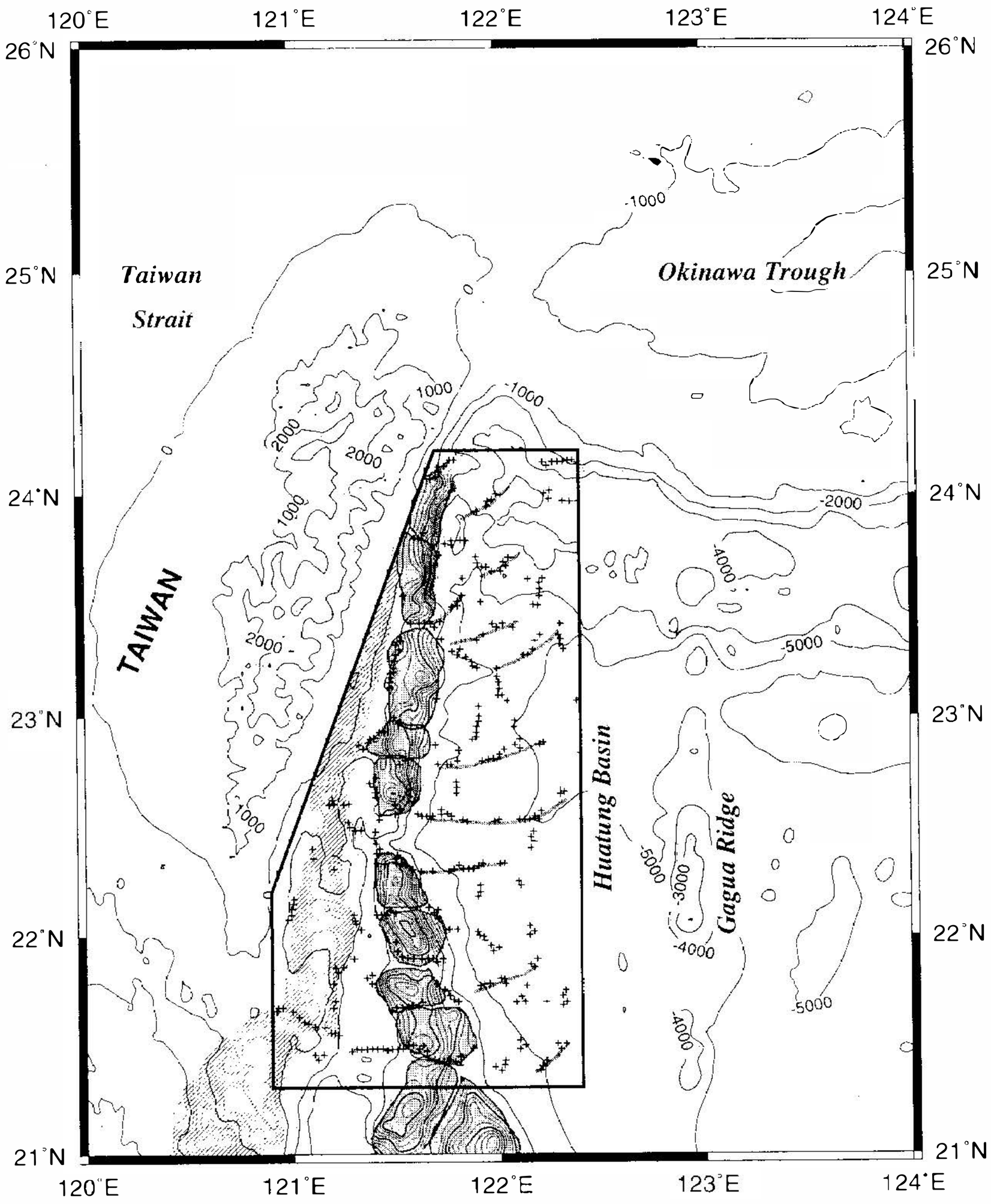

Fig. 7. Delineated magnetic basement (gray areas) corresponding to the northern portion of the Luzon Arc. The automatically detected structural boundaries are marked by "+" symbols. It is noted that the detected lineations (lines along the "+" symbols) are oriented E-W to NEE-SWW .

The distribution of earthquake epicenters with magnitudes greater than 4 from 1991 to 1996 in the Taiwan region is shown in Figure 8. Except for the earthquake distribution around the southernmost Ryukyu Arc and Okinawa Trough which are subduction-related, the earthquakes located to the east of the Longitudinal valley are pronounced (Figure 8). This directly implies that the Tananao Complex exhibits greater strength than the Luzon Arc. In fact, Sibuet

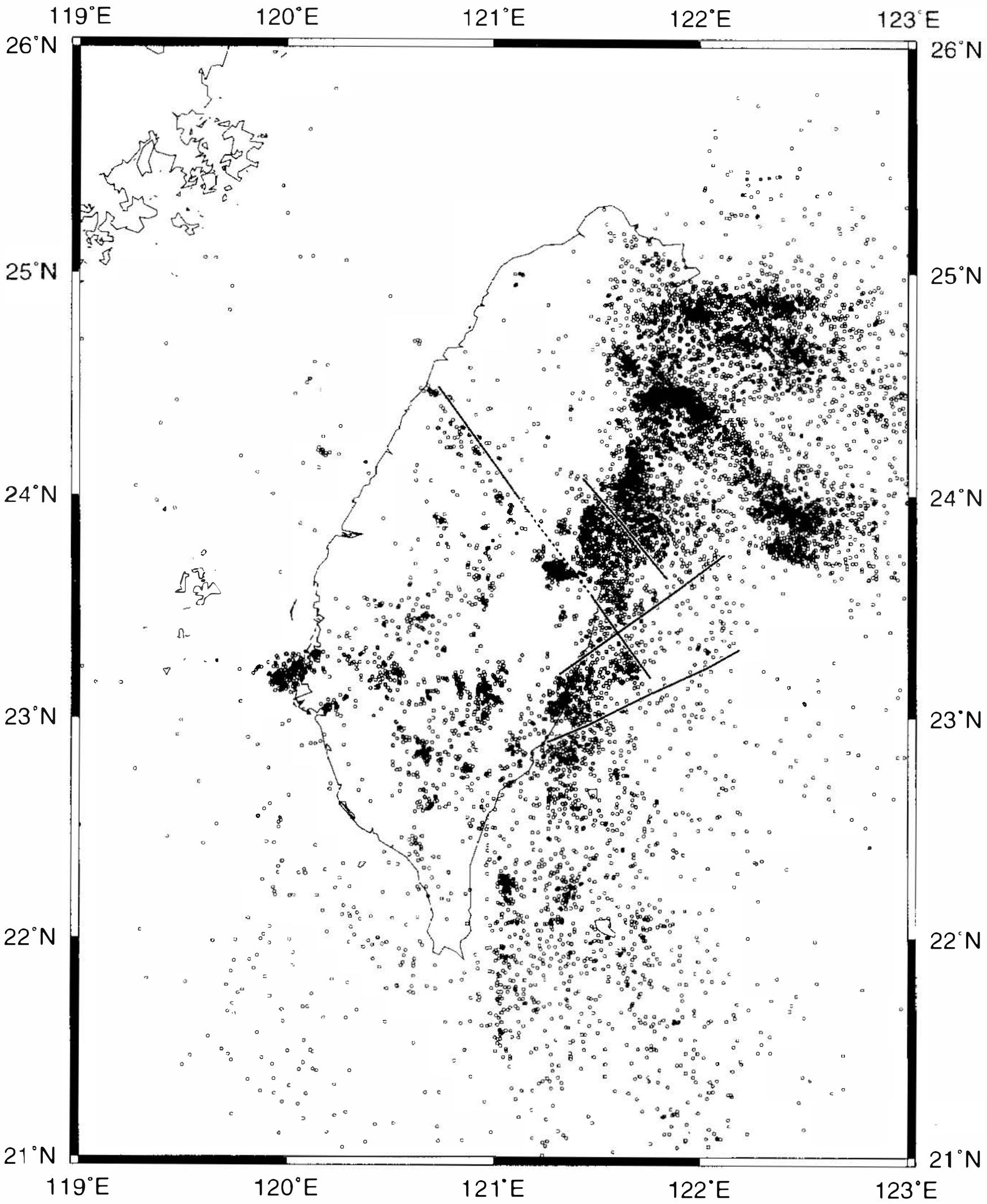

Fig. 8. Distribution of earthquake epicenters with magnitudes greater than 4 from 1991 to 1996. Note that the magnetic boundaries (black lines) determined by the analytic signal technique (Figure 7) are consistent with those of the distinctive earthquake provinces. The northwestward prolongated boundary from one of the determined boundaries across Taiwan is parallel to the direction of convergence of the Philippine Sea plate.

and Hsu (1996) and Cheng *et al.* (1996a) have demonstrated that the Luzon Arc is probably weaker than the Tananao Complex. A comparison of several magnetic boundaries with earthquake distribution (Figure 8) reveals that the proposed boundaries separate the earthquakes into several distinctive provinces surprisingly well. One of the detected boundaries may be related to the strike of an earthquake belt located in western Taiwan because its strike is in the

same direction and is parallel to the direction of convergence of the Philippine Sea plate relative to the Eurasian plate (Figure 8). It is worth noting that the two northernmost blocks of the Luzon Arc closely collide with the Tananao Complex (Figure 7), which implies a hard arc-arc collision as evidenced by the intensive occurrence of earthquakes in that area (Figure 8). A collisional bending effect (Wang, 1988) might in fact be associated with such a hard collision. To the south of the hard collision area, the collision between the Tananao Complex and the Luzon Arc is buffered by the compressed subduction complex and may correspond to a soft collision.

Since the Luzon Arc and the Tananao Complex generally exhibit stronger competence with respect to the compressed subduction complex in between (Figure 7), the compressed subduction complex could be regarded as an incompetent stripe. Due to the left-lateral motion between the Luzon Arc and the Tananao Complex, the compressed subduction complex may have been dragged so that the main geological structures of the Coastal Range orient NE-SW.

4. DEPTHS OF THE MAGNETIC BASEMENT

Based on the assumption that the shape of the power-density spectrum of the magnetic anomaly produced by a buried uniformly magnetized rectangular prism is in large part controlled by the average depth of the ensemble, Spector and Grant (1970) found that the spectrum decays exponentially with wavenumber at a rate of decay proportional to the average depth of the ensemble. Typical examples of the application surprisingly indicate that this simple and straightforward method could provide geologically reasonable solutions (e.g., Smith *et al.*, 1974; Blakely, 1988). Garcia-Abdeslem and Ness (1994) further modified the above interpretational scheme by proposing that other parameters of the magnetic ensemble (like thickness and horizontal dimension other than depth) also contribute to the overall shape of the spectrum and should be used in the interpretation. They verified the approach with numerical examples and concluded that the estimation of the average depth to the source may be incorrect if only the depth factor is considered , particularly when the low-wavenumber part of the spectrum is used. They applied the proposed method to magnetic data collected from offshore of the Yucatan Peninsula, Mexico and found it satisfactory.

Following this approach and assuming that the crustal magnetic anomaly is caused by an ensemble of vertical-sided and uniformly magnetized prisms, we selected six regions to estimate the depths to the top of the northern Luzon Arc by using the power spectrum method of Garcia-Abdeslem and Ness (1994) (Figure 9). Each selected region is 0.5^{o}x0.5^{o} (containing 50x50 grids). For modeling the spectrum, a Gaussian (normal) distribution was used to describe depth to the source top and a uniform distribution to describe the horizontal dimensions and the thickness function. Figure 10 shows the natural logarithm of the radially averaged and normalized power spectrum obtained from the magnetic anomaly shown in Figure 5 (in circles) and that from the iteratively inversed source model (in solid lines) for each of the six regions. The results of the previous experimental examples show that the technique has a better control on the solution of the depth and its standard deviation. Only the depth results are indicated in Figure 10. In general, the fitting is better in the low-wavenumber part of the spectrum which is better for depth estimation. On average, the magnetic basement associated with the Luzon Arc in the northern portion off eastern Taiwan is about 2 km in depth. The top of the magnetic

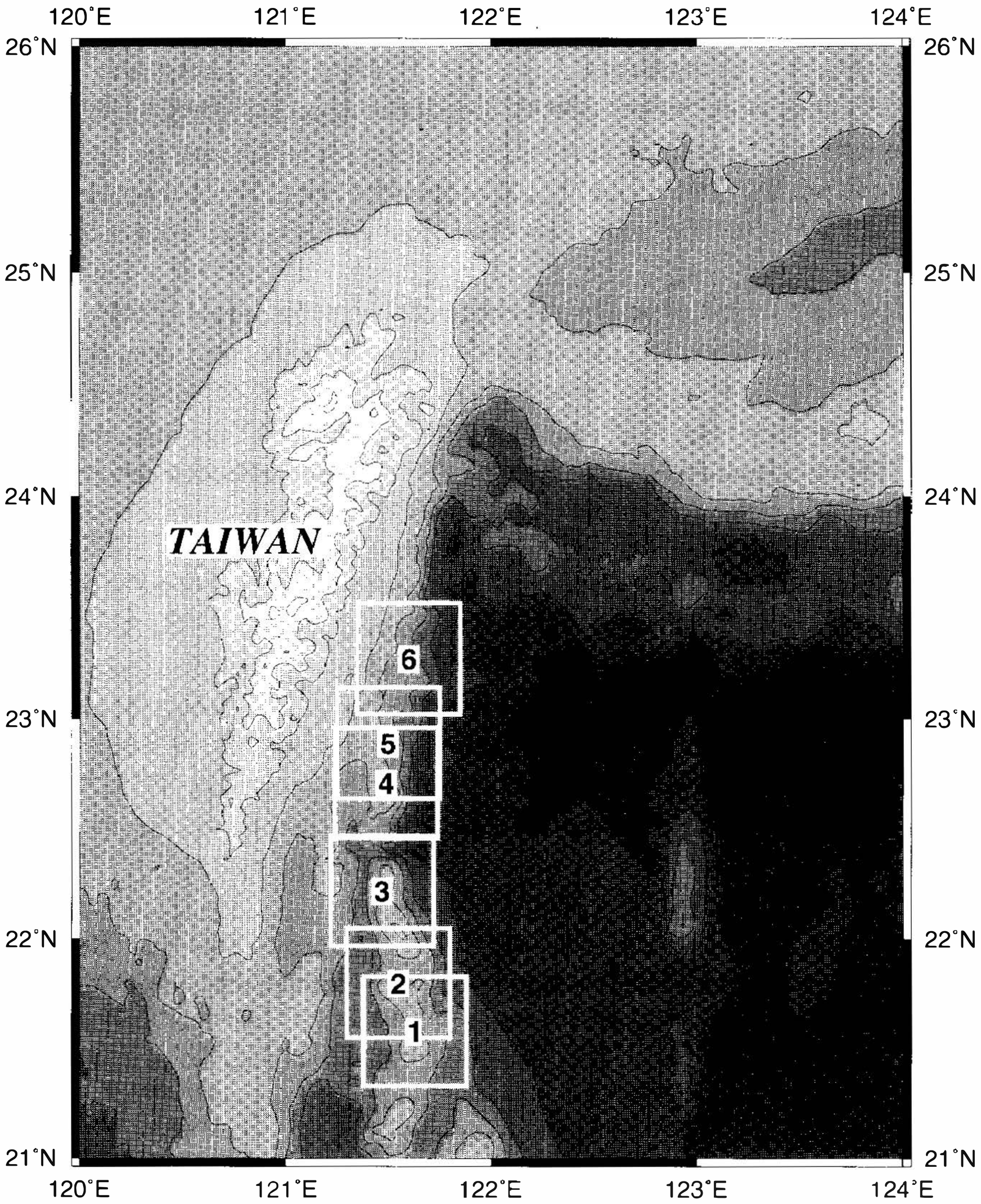

Fig. 9. Six regions of the northern Luzon Arc were selected for depth estimation by the power spectrum of the magnetic anomaly. Depths to the top of the magnetic basement are 2.23, 2.17, 2.21, 1.63, 2.14 and 2.25 km from Regions 1 to 6, respectively.

basement is 2.23 km in the most southern region rising to 2.17 km in Region 2 and again slightly deepening to 2.21 km in Region 3. North of the valley, it deepens northward from 1.63 km in Region 4, 2.14 km in Region 5 to 2.25 km in Region 6. By combining the magnetic basement boundary analysis with the present depth estimations, the northward extension of the Luzon Arc (composed typically of volcanic islands of andesitic breccia, basalts and tuff which produce the significant magnetic anomaly) shows that it has started subsiding. This is probably associated with the northwestward subduction of the Philippine Sea plate beneath northeastern Taiwan.

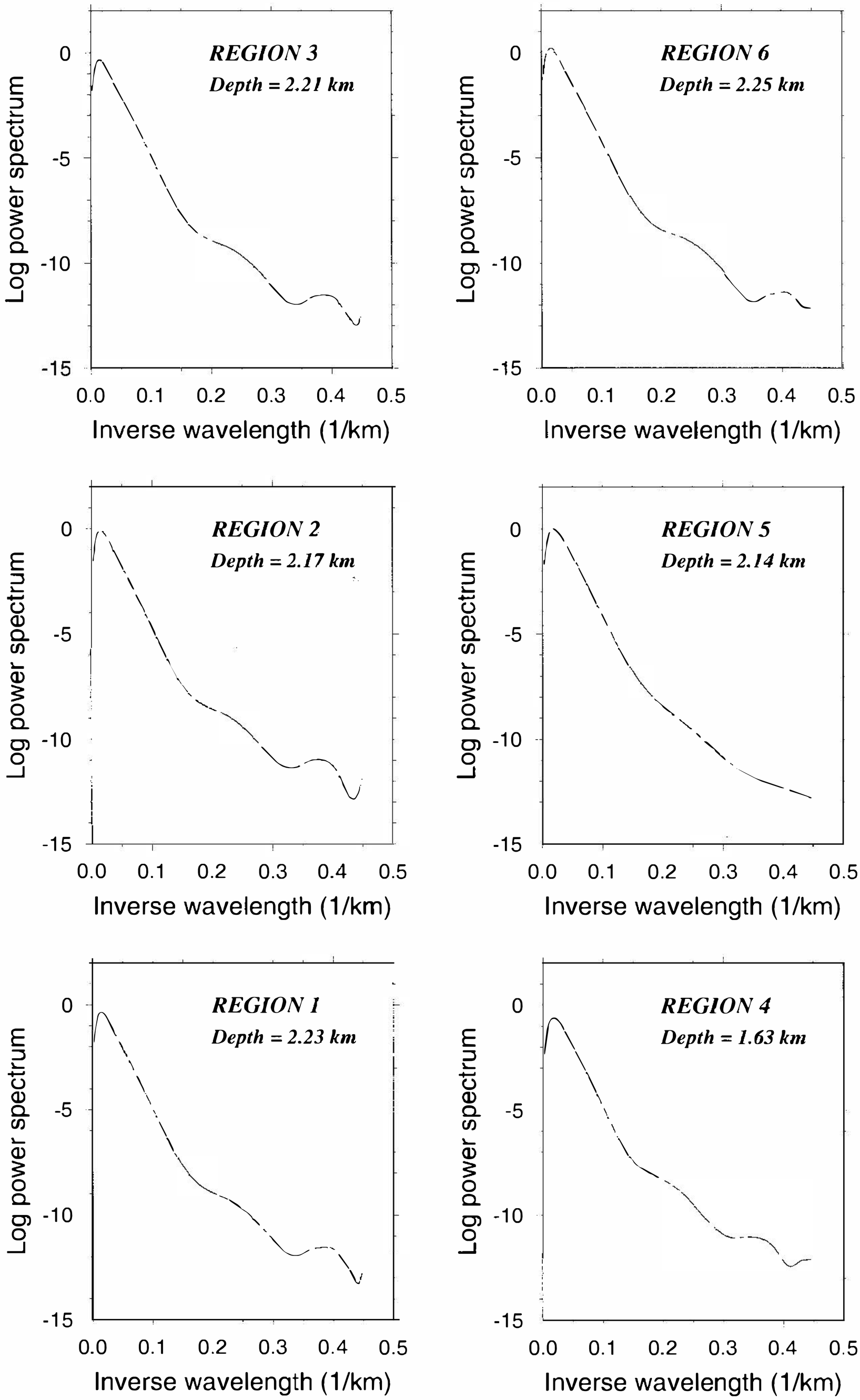

Fig. 10. Discrepancy between the natural logarithm of the radially averaged and normalized power spectrum (circles) from the magnetic anomaly shown in Figure 5 and that from the iteratively inversed source model (solid lines) for the six regions in Figure 9. The estimated depth to the magnetic source top of each region is indicated.

5. CONCLUSIONS

Magnetic data collected between 1989 and 1994 in the offshore area of eastern Taiwan were compiled. The outline of the magnetic sources was delineated with the help of the second-order enhanced analytical signal technique (Hsu *et al.*, 1996b) and the depths to the top of the magnetic source were estimated by the power spectrum method of Garcia-Abdeslem and Ness (1994).

It was found that the magnetic features corresponding to the existence of the northern Luzon Arc extend to the further east of the Coastal Range than previously considered and extend northward up to 24.18°N and 121.77°E. The northern Luzon Arc changes in orientation from NNW-SSE to NNE-SSW at the Taitung Canyon between Lutao and Lanhsu Islands. When the magnetic basement boundaries were compared with earthquake distribution in eastern Taiwan and its offshore area, the earthquakes could be separated into several distinctive regions limited by the detected magnetic boundaries. The collision at the northernmost Luzon Arc corresponds to a hard collision between the Luzon and the Tananao Complex, while to the south of 23.5°N, the collisional region corresponds to a soft collision. Most of the Coastal Range and the Huatung Ridge could be regarded as a compressed subduction complex (incompetent material between the Luzon Arc and the Tananao Complex).

The average depth to the top of the magnetic basement of the northern Luzon Arc is about 2 km. North of 22.7°N the magnetic basement of the Luzon Arc generally deepens towards the north, which suggests that the northernmost portion of the Luzon Arc has probably been subsiding.

Acknowledgment The authors thank the officers and crew of the *R/V Ocean Researcher I* and the R/V Professor Gagarinsky for bathymetric and magnetic data collection. The study was supported by the National Science Council of the Republic of China, under grants NSC 83-0202-M-002A-020, NSC 84-2011-M-002A-021 and NSC85-2611-M-002A-004.

REFERENCES

Blakely, R. J., 1988: Curie-temperature isotherm analysis and tectonic implications of aeromagnetic data from Nevada. *J. Geophys. Res.*, **93**, 11817-11832.

Blakely, R. J., and R.W. Simpson, 1986: Approximating edges of source bodies from the magnetic of gravity anomalies. *Geophysics*, **51**, 1494-1498.

Cheng, W.-B., C. Wang, and C.-T. Shyu, 1996: Crustal structure of the northeastern Taiwan area from refraction data. Proc. Geological Conference in memory of Prof. T. P. Yen, Chungli, 1996, 103-110.

Fuh, S.-C., C.-S. Liu, and G.-S. Song, 1994: Decoupled transcurrent faults in the offshore area south of Taiwan. *Petrol. Geol. Taiwan*, **29**, 27-46.

Garcia-Abdeslem, J., and G. E., Ness, 1994: Inversion of the power spectrum from magnetic anomalies. *Geophysics*, **59**, 391-401.

Ho, C.-S., 1988: An introduction to the geology of Taiwan: Explanatory text of the geologic map of Taiwan, 2nd. Ed., Ministry of Econ. Affairs, Rep. of China, 192pp.

Hsu, S.-K. and J.-C. Sibuet, 1995: Is Taiwan the result of arc-continent or arc-arc collision?. *Earth Planet. Sci. Lett.*, **136**, 315-324.

Hsu, S.-K., J.-C. Sibuet, S. Monti, C.-T Shyu, and C.-S. Liu, 1996a: Transition between the Okinawa Trough backarc extension and the Taiwan collision: new insights on the southernmost Ryukyu subduction zone. *Mar. Geophys. Res.*, **18**, 163-187.

Hsu, S.-K., J.-C. Sibuet, and C.-T. Shyu, 1996b: High-resolution detection of geologic boundaries from potential field anomalies: an enhanced analytic signal technique. *Geophysics*, **61**, 373-386.

Huang, C. Y., C. T. Shyu, S. B. Lin, T. Q. Lee, and D. Sheu, 1992: Marine geology in the arc-continent collision zone off southeastern Taiwan: Implications for Late Neogene evolution of the Coastal Range. *Mar. Geol.*, **107**, 183-212.

Huang, C. Y., P. B. Yuan, S. R. Song, C. W. Lin, C. Wang, M. T. Chen, C. T. Shyu, and B. Karp, 1995: Tectonics of short-lived intra-arc basins in the arc-continent collision terrane of the Coastal Range, eastern Taiwan. *Tectonics*, **14**, 19-38.

Kizaki, K., 1986: Geology and tectonics of the Ryukyu islands. *Tectonophysics*, **125**, 193-207.

Lu, C.-Y., and K. J. Hsu, 1992: Tectonic evolution of the Taiwan mountain belt. *Petrol. Geol. Taiwan*, **27**, 21-46.

Shyu, C.-T., and S.-C. Chen, 1991: A topographic and magnetic analysis off southeastern Taiwan. *Acta Oceano. Taiwan*, **27**, 1-20.

Sibuet, J.-C., and S.-K. Hsu, 1996: Geodynamics of the Taiwan arc-arc collision. *Tectonophysics* (in press).

Smith, R. B., R. T. Shuey, R. O. Freidline, R. M. Otis, and L. B. Alley, 1974: Yellowstone hot spot: New magnetic and seismic evidence. *Geology*, **2**, 451-455.

Spector, A., and F. S., Grant, 1970: Statistical models for interpreting aeromagnetic data. *Geophysics*, **35**, 293-302.

Suppe, J., 1981: Mechanics of mountain building and metamorphism in Taiwan. *J. Geol. Soc. China*, **4**, 67-89.

Suppe, J., 1984: Kinematics of arc-continent collision, flipping of subduction, and backarc spreading near Taiwan. *J. Geol. Soc. China*, **6**, 21-34.

Teng, L. S., 1990: Geotectonic evolution of late Cenozoic arc-continent collision in Taiwan. *Tectonophysics*, **183**, 57-76.

Wang, C., 1988: Horizontal lithospheric bending in the eastern Taiwan region. Proc. the Second Taiwan Symposium on Geophysics, 343-349.

Yu, S.-B., H. Y. Chen, and L.-C. Kuo, 1995: Velocity field of GPS stations in the Taiwan area. The international conference and 3rd Sino-French symposium on Active Collision in Taiwan, Taipei, March, 1995, 317-327.